

Performance Evaluation of Multi-Port Solar and PMSG Wind Based PFC Boost Converter with DTC Fuzzy Logic Scheme for Four-Switch Inverter Fed Induction Motor Applications

¹M. Hemachandran and ²R. Madhusudhanan

¹St. Peters University Avadi,

²Department of Electrical Engineering,
Sakthi Mariamman Engineering College, Thandalam, Chennai, India

Abstract: This study proposes, the multi-port power electronics PFC boost converter has attracted special interest in Four-Switch Three-Phase Inverter (FSTPI) drives by induction motor drives application. The proposed FSTPI scheme is used to eliminating two-switches of the conventional Six-Switch Three-Phase Inverter (SSTPI) which is controlled by using Direct Torque Control (DTC) with fuzzy logic controller. Multi-port power electronic converter has integrating solar with MPPT based boost converter for high step-up application and PMSG wind based three-phase, single-switch, Power Factor Correction (PFC) rectifier is can achieve less Total Harmonic Distortion (THD) power conversion system. The single-switch based PFC converter has higher efficiency and low common-mode EMI noise due to soft-switching operation. FSTPI approach has been adopted in the design of the vector selection table of the proposed DTC strategy which considers a subdivision of the Clarke plane into 6 sectors. The fuzzy logic controller is implemented using the direct torque control technique, as it provides better control of motor torque with high dynamic performances are verified by using various tool boxes in Matlab.

Key words: PV array, MPPT, PMSG wind, boost converter, power factor correction, THD, fuzzy logic control, Induction Motor (IM), Direct Torque Control (DTC), Four-Switch Three-Phase Inverter (FSTPI)

INTRODUCTION

In recent years for high power industrial applications, the Direct Torque Control (DTC) strategies have been widely implemented and achieves desirable speed due to dynamic response of AC drives. DTC strategy is a simple control scheme and which can involves to make a rapid real time implementation (Chen *et al.*, 2013). Since, several investigations carried out in order to improve the performance of the original DTC strategy. The major focused features are the uncontrolled switching frequency of the inverter and the high torque ripple resulting from the use of flux and torque. Currently, more DTC strategies has investigated (Zhang and Zhu, 2011). Those are classified in 4 categories:

- Variable hysteresis band controllers are considered (Kang *et al.*, 1999)
- Strategies with Space Vector Modulation (SVM)-based control of the switching frequency (Beerten *et al.*, 2010; Zhu *et al.*, 2012)
- Predictive control schemes are used (Kolar and Friedli, 2011)

- Strategies built around intelligent control approaches (Hassan *et al.*, 1991)

The proposed DTC scheme has decades of investigated by intelligent fuzzy logic controlling algorithm. Traditional PI based DTC scheme should produces outer speed loop because of the simplicity and less stability, however unexpected load change conditions or environmental factors would produce overshoot, oscillation of motor speed, oscillation of the torque, long settling time and thus causes deterioration of drive performance. To overcome this, an intelligent controller based on fuzzy logic can be used in the place of PI regulator (Uddin *et al.*, 2002).

Commonly, Voltage Source Inverter (VSI) feeding IM is have been arranged by 3 legs with Six-Switches in Three-Phase Inverter (SSTPI). This said some applications, such as electric and hybrid propulsion systems should be as reliable as possible. Within this requirement which reduces the switching losses and the reconfiguration of the SSTPI into a Four-Switch Three-Phase Inverter (FSTPI), in case of a switch/leg failure is currently given an increasing attention (Kolar

and Friedli, 2011). This FSTPI fed IM drive is penalized by the low dynamic and offer high performance in terms of torque ripple reduction allied to the control of the inverter switching losses. However, these performances are compromised by the complexity of their implementation schemes.

Additionally, the solar and wind energy based multi-port boost converters are associated with FSTPI fed IM drive which is produced the input DC supply to inverter side. The output power of a solar array depends on the operating terminal voltage where using of MPPT is insulates with temperature and improve the efficiency of PV array, the maximum tracking power is associated with DC-DC converter.

PMSG based wind energy generation is another port of multi-port system. The proposed three-phase single-switch Power Factor Correction (PFC) rectifier is reveal of superior power factor correction and Total Harmonic Distortion (THD) which is compared with conventional methods (Kolar and Friedli, 2011). To improve the input side THD of the three-phase single-switching rectifier were introduced by Zhang *et al.* (2012). In the proposed single-switch based rectifier can reduced the line THD as <5%.

This study proposes a new, wind based three-phase, single-switch with split capacitor approach is manipulate to eliminates a high-voltage-rated components and achieves superior THD and PFC boost rectifier is introduced. The PFC boost rectifier can achieves <5% input current THD without using any additional soft-switching circuits. Besides, the rectifier automatically achieves balancing between the voltages of the 2 series capacitors connected in output side. In addition, solar with MPPT boost converter is also successfully associated with wind power generation system which is produced efficient DC source to propose FSTPI fed IM drive. The Four-switch inverter is controlled by using DTC fuzzy logic controller. The proposed scheme makes more application.

PROPOSED SYSTEM

The proposed block diagram is shown in Fig. 1.

Photovoltaic array with boost converter: The electric power supplied by using multi-port converters one is radiation and temperature based solar photovoltaic power generation system is becoming increasingly important source, since it offers more merits such as incurring no fuel costs not being pollution, requiring low maintenance. PV array is still have relatively control by using Maximum

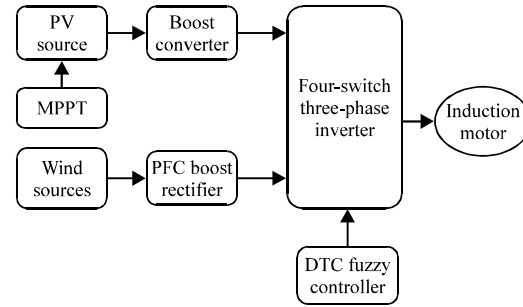


Fig. 1: Proposed block diagram

Power Point Tracking (MPPT) is achieves efficient system. A PV's Maximum Power Pint (MPP) varies with solar insulation and temperature. Maximum power delivery is depends upon the 5-1 characteristic unique operating point. At the PP, the PV operates at highest efficiency. Therefore, many methods have been developed to determine MPPT. The 5-1 characteristics of a PV array is given by Eq. 1 (Bose *et al.*, 1985):

$$I = I_{sc} - I_0 \left\{ \exp \left[\frac{q(V + R_s I)}{nkT_k} \right] - 1 \right\} - \frac{V + R_s I}{R_{sh}} \quad (1)$$

Where:

- V = The output voltage of the PV
- I = The current of the PV
- R_s = The series resistance of the cell
- R_{sh} = The shunt resistance of the cell
- q = The electronic charge
- I₀ = The reverse saturation current
- n = The dimensionless factor
- k = The Boltzman constant
- T_k = Temperature

Wind power generation: The basic principle of wind turbine is linear motion into rotational energy. An electrical generator is performed by rotational energy, allowing the wind kinetic energy to be turned into electric power (Zhu *et al.*, 2012).

The captured power of the wind (P_v) for wind turbine is given by Eq. 2:

$$P_v = \frac{1}{2} \cdot \rho_a \cdot A_v \cdot u^3 \quad (2)$$

Where:

- ρ_a = Wind velocity
- u = Wind speed
- A_v = Wind turbine area of swept

The mechanical power (P_m) is generated by the wind turbine from the capture power of wind depends of the power coefficient (C_p) of the wind turbine, as it shows the Eq. 3:

$$P_m = P_v \cdot C_p(\lambda) \quad (3)$$

Tip-speed ratio λ , given C_p is the tip speed ratio λ , given by Eq. 4:

$$\lambda = \frac{r \cdot \omega_m}{n} \quad (4)$$

Where:

r = The length of the wind turbine spade

ω_m = The angular rotor speed

PMSG wind model: The proposed Permanent Magnet Synchronous Generator (PMSG) which is constructed by using number of poles to avoid the availability of gearbox, presents of PMSG have some advantages when compared with the DFIG in Wind Energy Conversion Systems (WECS) (Beerten *et al.*, 2010). External excitation current is not required, such as light weight, compact size, more reliability, good efficiency. Effective mechanical torque (T_m) is applied to the PMSG is given by:

$$T_m = \frac{P_m}{\omega_m} \quad (5)$$

$$T_m = \frac{1}{2} \cdot \rho_a \cdot A_v \cdot \frac{C_{pr}}{\lambda} \cdot u^2 \quad (6)$$

$$T_e = \frac{E_a \cdot I_a + E_b \cdot I_b + E_c \cdot I_c}{\omega_m} \quad (7)$$

Where, T_e is the electromagnetic torque of the PMSG power generation unit.

Wind based PFC boost rectifier: Proposed three-phase single-switch PFC boost rectifier provided effective neutral potential balance the three Y-connected capacitors, C_1 - C_3 are used to create virtual neutral N, i.e., same potential there is no physical connection in three-wire power systems. Since, the effective neutral is connected to the midpoint between switch S_1 and capacitor voltage same as in neutral point of three-phases. In addition by connecting virtual neutral N directly to the midpoint between switch S_1 and capacitor, decoupling of the 3 input currents is achieved. In each decoupled inductor circuit current depends on phase voltage of each phases, current reduces the THD and increases the PFC (Chen *et al.*, 2013). The measured THD values are better which is compared to conventional two-switch based boost rectifier.

DTC of FSTPI-Fed IM drives: DTC strategies should allows to estimates the torque and flux from voltage and current. Direct control of the inverter is used to limits the torque and flux errors. Direct torque control is a strategy for induction motor speed adjustment fed by variable frequency converter. These decision can achieves the output of flux ($C\phi$) and torque ($C\tau$) hysteresis controller, respectively and θ_s is angular displacement, Φ_s is the stator flux vector of the the Clarke ($\alpha\beta$) plane.

The dynamic value of Φ_s is governed by the stator voltage equation expressed in the stationary reference frame, as follows:

$$\frac{d}{dt} \Phi_s = V_s - r_s I_s \quad (8)$$

Where, V_s , I_s and r_s are represented by stator voltage, current, resistance. Voltage drop of across the stator resistance $r_s I_s$ is neglected. T_s is sampling period. Where, V_s , I_s and r_s are the stator voltage vector, current vector and resistance, respectively. If the stator flux is kept constant and its angle is changed, at fast the electromagnetic torque is controlled directly. The reference values of stator flux and torque values are compared with their actual values (Zhu *et al.*, 2012). The induced electromagnetic Torque (T_{em}) of induction motor is derived by the equation and it can depends on the direction of the applied voltage vector:

$$T_{em} = N_p \frac{M}{l_r l_s - M^2} \|\Phi_s\| \|\Phi_r^*\| \sin \delta \quad (9)$$

Where:

Φ_r^* = The rotor flux vector which is represented by stator
 δ = The angular shift between the stator and rotor fluxes

N_p = The pole pair number

l_r = The stator self-inductance

l_s = The rotor self-inductance

M = The mutual inductance

The proposed FSTPI fed IM topology consists of a 3 legs arrangement. Where first 2 legs are made by using ($S_{1,4}$) switches while the third leg is connected between the 2 DC link capacitors where the ON/OFF states of the switches are denoted by the binary variables where the binary 1 indicates an ON state and the binary 0 represents an OFF state:

$$\begin{bmatrix} V_{as} \\ V_{bs} \\ V_{cs} \end{bmatrix} = \frac{V_{dc}}{6} \begin{bmatrix} 4 & -2 & -1 \\ -2 & 4 & -1 \\ -2 & -2 & 2 \end{bmatrix} \begin{bmatrix} S_1 \\ S_2 \\ 1 \end{bmatrix} \quad (10)$$

$$\begin{bmatrix} V_{\alpha s} \\ V_{\beta s} \end{bmatrix} = \frac{\sqrt{2}}{\sqrt{3}} \begin{bmatrix} 1 & -1/2 & -1/2 \\ 0 & \sqrt{3}/2 & -\sqrt{3}/2 \end{bmatrix} \begin{bmatrix} V_{as} \\ V_{bs} \\ V_{cs} \end{bmatrix} \quad (11)$$

About 4 combinations of the states of the upper switches are distinguished by 4 active voltage vectors (V_{1-4}) in the plane $\alpha\beta$ which is shown in Table 1. The 4 active voltage vectors denoted in the $\alpha\beta$ plane which is shown in Fig. 2. The 4 vectors have unbalanced amplitudes and these are shifted by the angle of $\pi/2$ as it happen, vectors V_1 and V_3 have an amplitude of $V_{DC}/6$ while vectors V_2, V_4 are have an amplitude of $V_{DC}/\sqrt{2}$ (Fig. 3).

Fuzzy logic control: In recent years, fuzzy logic control, as a powerful tool and fuzzy logic algorithm has

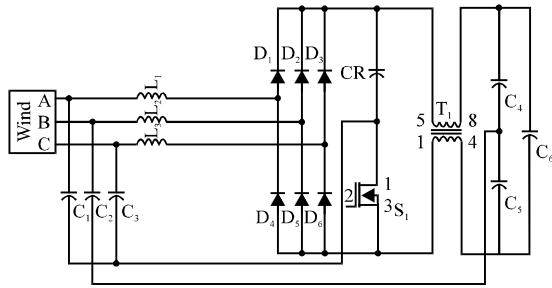


Fig. 2: Wind based single-switch rectifier

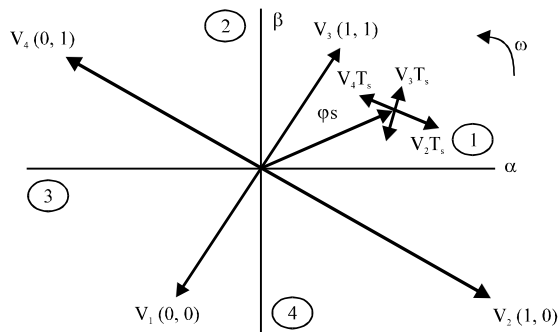


Fig. 3: Unbalanced active voltage vectors generated by the FSTPI

Table 1: Fuzzy control rules

de/e	LN	MN	SN	Z	SP	MP	LP
LN	LP	LP	LP	MP	MP	SP	Z
MN	LP	MP	MP	MP	SP	Z	SN
SN	LP	MP	SP	SP	Z	SN	MN
Z	MP	MP	SP	Z	SN	MN	MN
SP	MP	SP	Z	SN	SN	MN	LN
MP	SP	Z	SN	MN	MN	MN	LN
LP	Z	SN	MN	MN	LN	LN	LN

implemented in many rules which is used in various power system applications (Khanna *et al.*, 2009). Such as a controlling technique application has been motivated by the following reasons:

- Compared to conventional linear control method fuzzy logic have better robustness
- Simplified control design for difficult system models
- Simplified implementation

Application of fuzzy techniques appears to be making the most suitable one. Sometimes, the well-defined linear control objective cannot be specified that is the system controller is complex one or mathematical model is not available. Recent research indicates that more emphasis has been placed on the combined usage of fuzzy systems and neural networks (Hassan *et al.*, 1991).

The fuzzy logic control algorithm involves 3 steps of fuzzification, application of fuzzy rules and decision making and defuzzification. Fuzzification involves mapping input crisp values to fuzzy variables. Where the input constraints were terminal voltage error and its variations; the output constraint was the increment of the voltage exciter. FLC are defined, as 2 input units where as error and change of error.

Fuzzy sets are defined for each input and output variable. There are 7 fuzzy levels (Large Negative (LN), Medium Negative (MN), Small Negative (SN), Zero (Z), Small Positive (SP), Medium Positive (MP), Large Positive (LP)) (Hassan *et al.*, 1991). The membership functions for input and output variable are triangular. The min-max method inference engine is used; the defuzzify method used in this FLC is centre of area. The complete set of control rules is shown in Table 1-4.

Table 2: Vector selection table of the basic DTC strategy

$C\varphi, C\tau$	+1, +1	+1, -1	-1, +1	-1, -1
1 sector	V_3	V_2	V_4	V_1
2 sector	V_4	V_3	V_1	V_2
3 sector	V_1	V_4	V_2	V_3
4 sector	V_2	V_1	V_3	V_4

Table 3: Circuit parameters for wind side PFC converter

Parameters	Values
L	200 uH
C	2.2 uF
C_R	3 uF
L_m	1.7 mH
L_k	145 uH
C_1, C_2	270 uF

Table 4: Induction machine parameters

Parameters	Values	Parameters	Values
Power	0.37 kW	r_s	24.6 Ω
Voltage	230/400 V	r_r	17.9 Ω
Speed	1000 rpm	l_s	984 mH
Torque	2.56 Nm	l_r	984 mH
Current	0.15 A	M	914 mH
Frequency	50 Hz	J	2.5 gm ²

SIMULATION RESULTS

Simulation model of multi-port solar and wind energy generation based boost converter and integration of fuzzy logic based DTC FSTPI fed induction motor drive has been developed by using

Simulink Matlab. The proposed Three-phase single-switch PFC boost rectifier has achieves <5% input current THD. The performance evaluation was performed on a Simulink, the measured input current at 290 and 380 VL-L, RMS were 2.9 and 3.48%, respectively (Fig. 4-10).

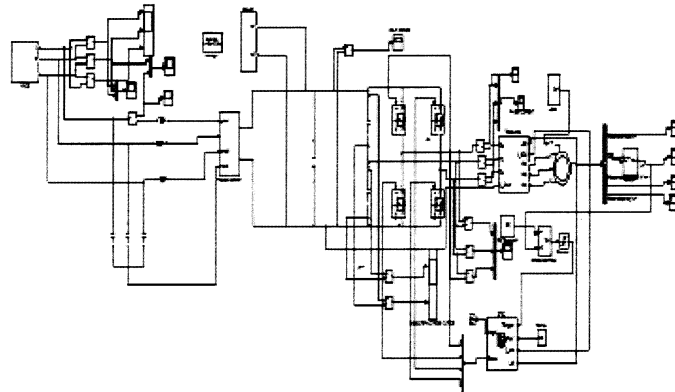


Fig. 4: Proposed circuit

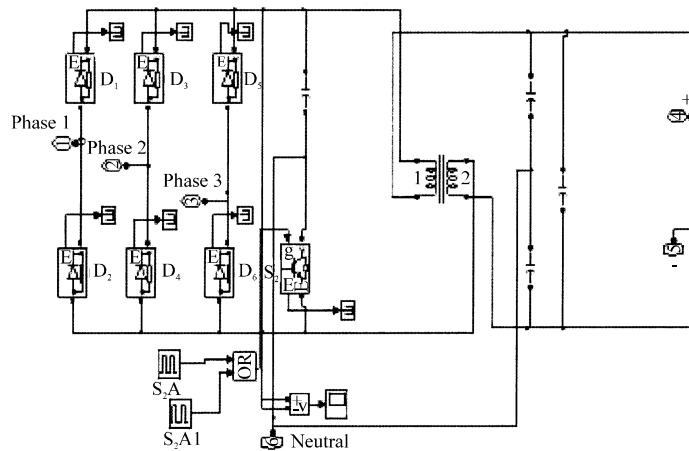


Fig. 5: Single-switch based boost rectifier circuit

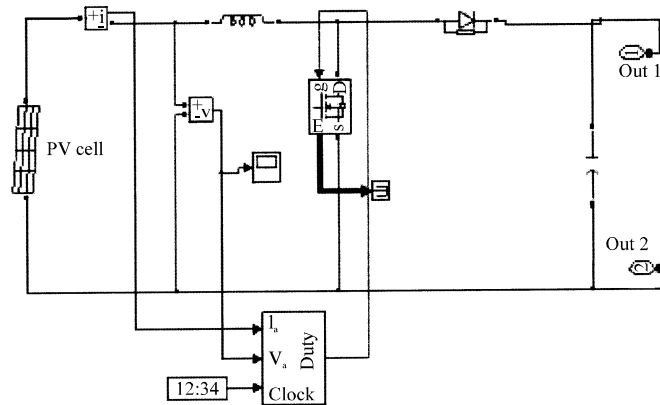


Fig. 6: PV array with converter circuit

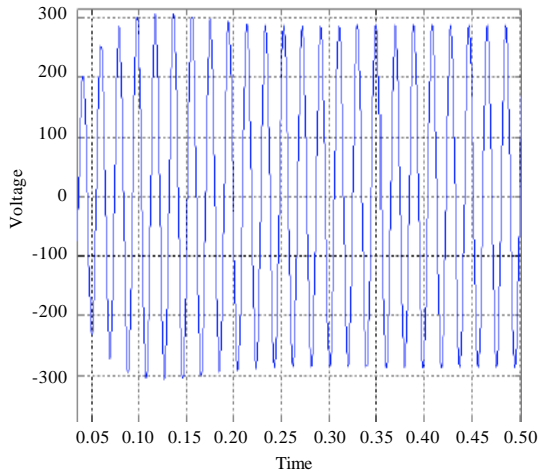


Fig. 7: Wind voltage

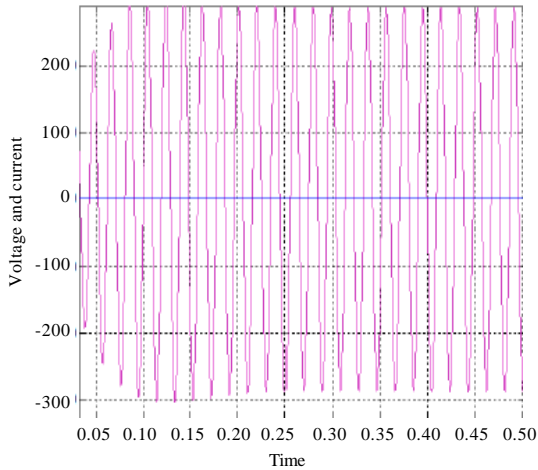


Fig. 8: Power Factor Correction (PFC)

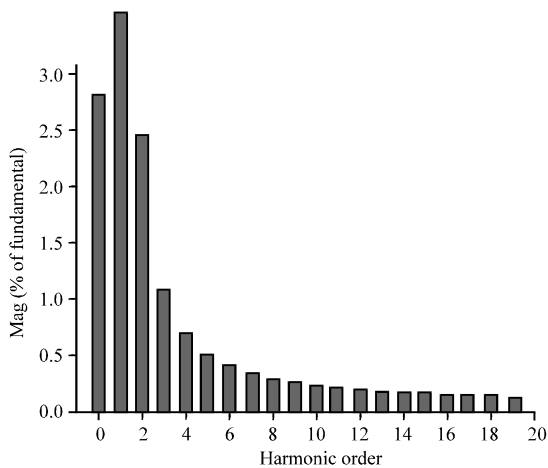


Fig. 9: Total Harmonic Distortion (THD); Fundamental (50 Hz) = 289.2; THD = 2.94%

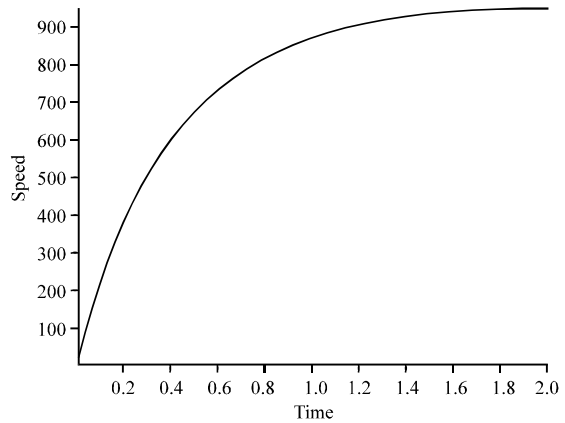


Fig. 10: Induction motor speed

CONCLUSION

In this study, the multi-port solar with MPPT based boost converter and PMSG wind energy PFC boost rectifier has attracted special interest in Four-Switch Three-Phase Inverter (FSTPI) drives by the induction motor drives application. The proposed FSTPI and the control strategy of novel direct torque control with fuzzy logic scheme is used to eliminating two-switches of the conventional Six-Switch Three-Phase Inverter (SSTPI) and achieves dynamic speed. The proposed three-phase single-switch PFC boost rectifier has achieves <5% input current THD. The performance evaluation was performed on a SIMULINK, the measured input current at 290 and 380 VL-L, RMS were 2.9 and 3.48%, respectively.

REFERENCES

Beerten, J., J. Vervecken and J. Driesen, 2010. Predictive direct torque control for flux and torque ripple reduction. *IEEE Trans. Ind. Electron.*, 57: 404-412.

Bose, B.K., P.M. Szczeny and R.L. Steigerwald, 1985. Microcomputer control of a residential photovoltaic power conditioning system. *IEEE Trans. Ind. Electron.*, IA-21: 1182-1191.

Chen, Y.M., A.Q. Huang and X.W. Yu, 2013. A high step-up three-port DC-DC converter for stand-alone PV/battery power systems. *IEEE Trans. Power Electron.*, 28: 5049-5062.

Hassan, M.A.M., O.P. Malik and G.S. Hope, 1991. A fuzzy logic based stabilizer for a synchronous machine. *IEEE Trans. Energy Convers.*, 6: 407-413.

Kang, J.K., D.W. Chung and S.K. Sul, 1999. Direct torque control of induction machine with variable amplitude control of flux and torque hysteresis bands. *Proceedins of the International Conference on Electric Machines and Drives*, May 1999, Seattle, Washington, pp: 640-642.

- Khanna, R. M. Singla and G. Kau, 2009. Fuzzy logic based direct torque control of induction motor. Proceedings of IEEE Power and Energy Society General Meeting, July 26-30, 2009, Calgary, Alberta, Canada, pp: 1-5.
- Kolar, J.W. and T. Friedli, 2011. The essence of three-phase PFC rectifier systems. Proceedings of the IEEE 33rd International on Telecommunications Energy Conference, October 9-13, 2011, Amsterdam, pp: 1-27.
- Uddin, M.N., T.S. Radwan and M.A. Rahman, 2002. Performances of fuzzy-logic-based indirect vector control for induction motor drive. IEEE Trans. Ind. Applic., 38: 1219-1225.
- Zhang, Y. and J. Zhu, 2011. Direct torque control of permanent magnet synchronous motor with reduced torque ripple and commutation frequency. IEEE Trans. Power Electron., 26: 235-248.
- Zhang, Y., J. Zhu, Z. Zhao, W. Xu and D.G. Dorrell, 2012. An improved direct torque control for three-level inverter-fed induction motor sensorless drive. IEEE Trans. Power Electron., 27: 1502-1513.
- Zhu, H., X. Xiao and Y. Li, 2012. Torque ripple reduction of the torque predictive control scheme for permanent-magnet synchronous motors. IEEE Trans. Ind. Electron., 59: 871-877.